Original Article

Potential Role of BNIP3 in Cardiac Remodeling, Myocardial Stiffness, and Endoplasmic Reticulum

Mitochondrial Calcium Homeostasis in Diastolic and Systolic Heart Failure

Antoine H. Chaanine, MD; Ronald E. Gordon, PhD; Erik Kohlbrenner, BS; Ludovic Benard, PhD; Dongtak Jeong, PhD; Roger J. Hajjar, MD

Background—We have shown that BNIP3 expression is significantly increased in heart failure (HF). In this study, we tested the effects of BNIP3 manipulation in HF.

Methods and Results—In a rat model of pressure overload HF, BNIP3 knockdown significantly decreased left ventricular (LV) volumes with significant improvement in LV diastolic and systolic function. There were significant decreases in myocardial apoptosis and LV interstitial fibrosis. Ultrastructurally, BNIP3 knockdown attenuated mitochondrial fragmentation and restored mitochondrial morphology and integrity. On the molecular level, there were significant decreases in endoplasmic reticulum (ER) stress and mitochondrial apoptotic markers. One of the mechanisms by which BNIP3 mediates mitochondrial dysfunction is via the oligomerization of the voltage-dependent anion channels causing a shift of calcium from the ER to mitochondrial compartments, leading to the decrease in ER calcium content, mitochondrial damage, apoptosis, and LV interstitial fibrosis, and hence contributes to both systolic and diastolic myocardial dysfunction, respectively. In systolic HF, the downregulation of SERCA2a (sarcoplasmic-endoplasmic reticulum calcium ATPase), along with an increased BNIP3 expression, further worsen myocardial diastolic and systolic function and contribute to the major remodeling seen in systolic HF as compared with diastolic HF with normal SERCA2a expression.

Conclusions—The increase in BNIP3 expression contributes mainly to myocardial diastolic dysfunction through mitochondrial apoptosis, LV interstitial fibrosis, and to some extent to myocardial systolic dysfunction attributable to the shift of calcium from the ER to the mitochondria and to the decrease in ER calcium content. However, SERCA2a downregulation remains a prerequisite for the major LV remodeling seen in systolic HF. **(*Circ Heart Fail*. 2013;6:572-583.)**

Key Words: apoptosis ■ gene therapy ■ heart failure ■ hypertrophy ■ remodeling

In heart failure (HF), the cross-talk between the endoplasmic reticulum–sarcoplasmic reticulum (ER/SR) and the juxtaposed mitochondria is altered, leading to the malfunction of the cardiomyocyte and to the decline in cardiac function. On the SR level, there is hyperphosphorylation of the ryanodine receptors, hypophosphorylation of phospholamban, downregulation and dysfunction of SERCA2a. These changes in the calcium cycling proteins lead to increases in SR Ca^{2+} release and to decreases in SR Ca^{2+} uptake, and SR Ca^{2+} content. On the mitochondrial level, there is an increase in the proapoptotic Bcl-2 and Bcl-2 like family proteins, such as Bax and BNIP3, respectively, in favor of the antiapoptotic marker Bcl-2. BNIP3 is a mitochondrial death and mitophagy marker that has been shown to induce left ventricular (LV) remodeling postmyocardial infarction.[1–9] In our previous study, we highlighted the role of c-Jun N-terminal kinases (JNK) in modulating FOXO3a (forkhead box transcription factors) for the expression of BNIP3 in pressure overload hypertrophy (POH) and in HF.[10] This signaling pathway was further validated in human samples of HF.[10] BNIP3 expression increased the first 2 weeks after POH and peaked at HF development.[10] In this study, we show how BNIP3 knockdown, using tail vein injection of adeno-associated virus of serotype 9 (AAV9) Sh BNIP3, reversed cardiac remodeling and improved LV diastolic and systolic function in a pressure overload rat model of diastolic and systolic HF. Moreover, BNIP3 knockdown robustly attenuated LV apoptosis and interstitial fibrosis with major improvements of various cellular components, specifically with regard to mitochondrial morphology and integrity. Mechanistically, we find that BNIP3 exerts its destructive effects on the mitochondria via the oligomerization of the voltage-dependent anion channel (VDAC), leading to mitochondrial Ca^{2+} overload, release of cytochrome C, and mitochondrial apoptosis as shown below.

Clinical Perspective on p 583

Received June 21, 2012; accepted March 1, 2013.

From the Cardiovascular Institute (A.H.C., E.K., L.B., D.J., R.J.H.), and Pathology Department (R.E.G.), Mount Sinai School of Medicine, New York, NY.

The online-only Data Supplement is available at http://circheartfailure.ahajournals.org/lookup/suppl//doi:10.1161/CIRCHEARTFAILURE.112.000200/-/DC1.

Correspondence to Roger J. Hajjar, MD, One Gustave L. Levy Place, Box 1030, New York, NY 10029. E-mail roger.hajjar@mssm.edu

Circ Heart Fail **is available at http://circheartfailure.ahajournals.org** **DOI: 10.1161/CIRCHEARTFAILURE.112.000200**

Methods

Isolation and Culture of Adult Rat Cardiomyocytes and In Vitro Experiments

Adult rat ventricular cardiomyocytes were isolated from male Sprague-Dawley rats weighing 250 to 350 g, as previously described.[11,12] The following experiments were performed (n=3 for each experiment in vitro): (1) cell viability, (2) mitochondrial membrane potential, (3) immunofluorescence staining, (4) mitochondrial Ca^{2+} loading (Figure I in the online-only Data Supplement), and (5) VDAC oligomerization. Details are available in the online-only Data Supplement.

Western Blotting

Please refer to the online-only Data Supplement.

Coimmunoprecipitation

The coimmunoprecipitation was performed using Pierce Classic IP Kit (Thermo Scientific, Rockford, IL). Details are available in the online-only Data Supplement.

Transmission Electron Microscopy

Samples were viewed under a transmission electron microscope (HITACHI H-7650, Tokyo, Japan). Details are available in the online-only Data Supplement.

Production of Recombinant Adenoviruses and Adeno-Associated Virus

Recombinant adenoviruses encoding green fluorescent protein was prepared as previously described.[13] Ad-BNIP3 and Ad-Sh BNIP3 were done at vector biolabs. We generated a recombinant cardiotropic AAV9, allowing for cardiomyocyte-targeted RNAi against BNIP3 (AAV9 Sh BNIP3) under control of the U6 promoter[14] (Figure II in the online-only Data Supplement).[14]

Apoptosis by Tunnel Staining

Tunnel staining was performed using the Apoptag red in situ detection kit (Millipore, Billerica, MA). Details are available in the online-only Data Supplement.

Masson Trichrome Staining

Cryosections were stained using Masson Trichrome staining kit protocol (Sigma, St. Louis, MO). Details are available in the online-only Data Supplement.

Measurement of Intracellular Calcium Kinetics and ER Calcium Content

Fura-2, AM (Molecular Probes, Eugene, OR) was used to detect intracellular Ca^{2+} concentration [Ca]i. Data are expressed as the 340:380 ratio after subtraction of background fluorescence. Details are available in the online-only Data Supplement.

Experimental Model of Ascending Aortic Banding, Cross-Clamp With Ascending Aortic Banding, and Study Design

All procedures involving the handling of animals were approved by the Animal Care and Use Committee of the Mount Sinai School of Medicine and adhered with the Guide for the Care and Use of Laboratory Animals published by the National Institutes of Health. Sprague-Dawley rats weighing 180 to 200 g underwent ascending aortic banding (AAB), as previously described in detail,[15] for the systolic HF model n=7 and for the diastolic HF model n=5 for each group. The cross-clamp surgery with gene transfer and AAB was performed as previously described in detail (n=4 for each group).[16,17] Details are available in the online-only Data Supplement.

Echocardiography

Transthoracic echocardiography was performed using a vivid 7 echocardiography apparatus with a 14-MHz probe (i13L probe, General Electric, New York, NY). Details are available in the online-only Data Supplement.

Invasive Pressure–Volume Loop Measurements of the LV

Hemodynamics were recorded using a Scisense P-V Control Unit (FY897B).[18–20] Details are available in the online-only Data Supplement.

Statistical Analysis

Results are shown as mean±SD. Statistical significance was determined using 1-way ANOVA followed by Tukey. There was no adjustment for multiple comparisons across the variables being tested. For the pretreatment and 1 month after treatment data, mixed effect models with a random intercept; treatment, time, and the interaction treatment * time were the predictors in the model. A significant interaction means that the change between before and after in either of the noncontrol groups was statistically different than the difference observed in the control group. A P value of <0.05 was considered statistically significant. The P values presented in the figures are 2 sided.

Results

BNIP3 Overexpression Induces Mitophagy and Apoptosis in Cardiomyocytes In Vitro and In Vivo and Impairs Diastolic and Systolic Cardiac Function in a Rat Model of Early POH

BNIP3 localizes to the mitochondria in cardiomyocytes (Figure IIIA in the online-only Data Supplement). BNIP3 overexpressing cardiomyocytes showed significant increases in cell death, cytoplasmic cytochrome C, and cleaved caspase 3, and significantly decreased mitochondrial membrane potential (Figure IIIB–IIID in the online-only Data Supplement).

Gene transfer of Ad-BNIP3 in a rat model of early POH was associated with a significantly lower body weight, LV weight, a significantly lower heart weight/body weight ratio, and a significantly thinner septal and posterior wall, by echocardiography (Figure 1A–1C; Table I in the online-only Data Supplement). There were significant increases in LV end-systolic diameters and volumes and significant decreases in LV fractional shortening and LV ejection fraction (LVEF) in the Ad-BNIP3 group (Figure 1D and 1E). Baseline hemodynamics and tracings are shown in Table II in the online-only Data Supplement and Figure 1F, respectively. The Ad-BNIP3 group had significant increases in their LV end-diastolic pressures, despite having a significantly lower maximum pressure and significantly decreased LVEF (Figure 1G–1I).

On the molecular level, there was no difference in SERCA2a expression among all groups. BNIP3 expression significantly increased in early POH (Ad-Null+AAB) and was further increased in the Ad-BNIP3 group (Figure 1J). The conversion of LC3-1 to LC3-2 and cleaved caspase 3 were significantly decreased in the Ad-Sh BNIP3 group (Figure 1J). Ultrastructurally, BNIP3 overexpression in pressure overload (PO) accentuated mitochondrial fragmentation and cristae destruction. BNIP3 knockdown robustly attenuated mitochondrial fragmentation and the presence of autophagosomes in PO (Figure 1K). Of note,

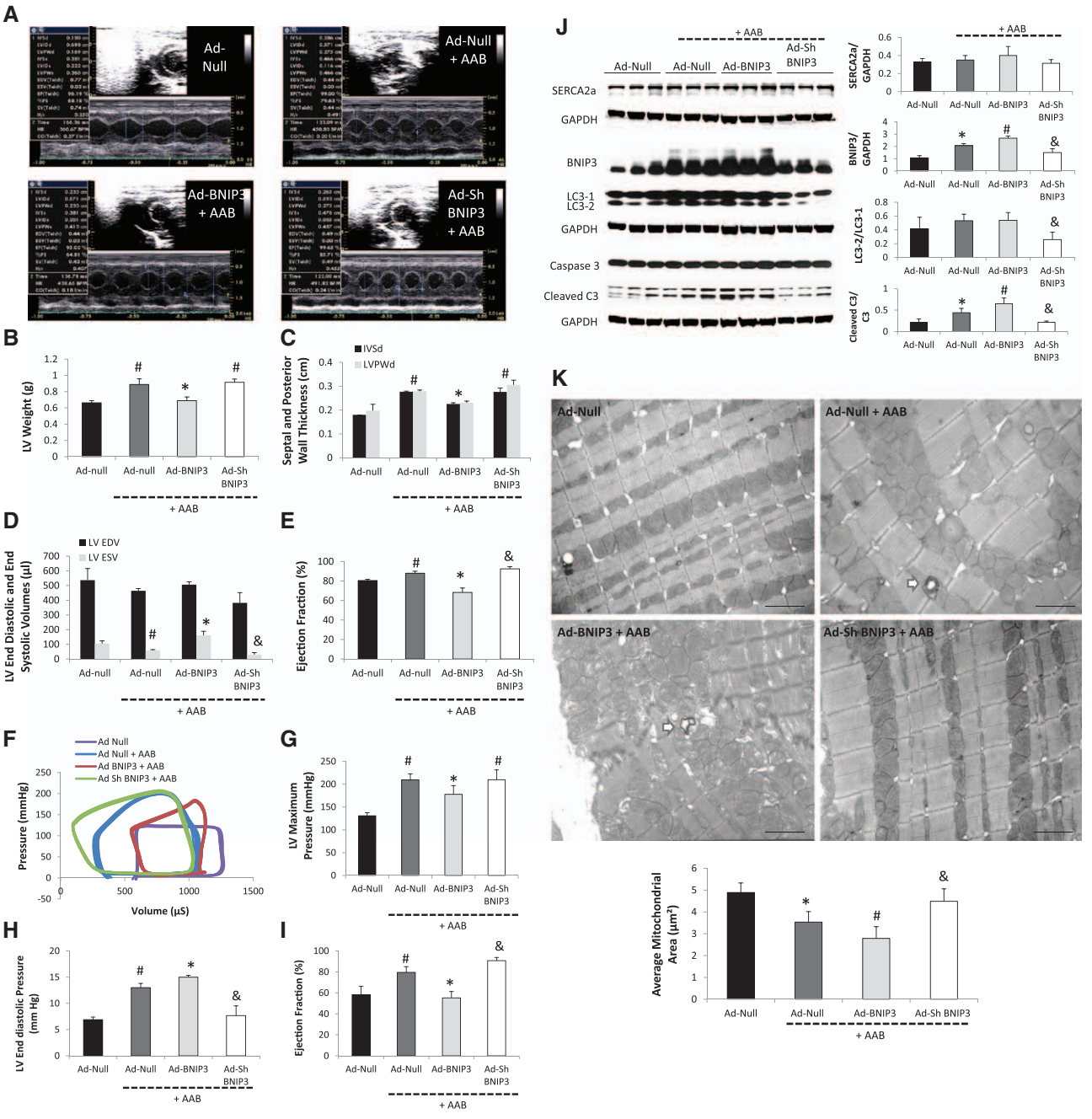

Figure 1. BNIP3 overexpression increased cardiomyocyte death in vitro and impaired LV systolic and diastolic function in a rat model of early pressure overload hypertrophy (POH). **A–E**, M-mode images 2 weeks after gene delivery via a cross-clamp technique and ascending aortic banding (AAB). There were significant decreases in left ventricular (LV) weight, interventricular septum thickness (IVSd), left ventricular end-diastolic posterior wall dimension (LVPWd), and left ventricular ejection fraction (LVEF), and significant increase in LV end-systolic volume in the Ad-BNIP3+AAB group, **P*<0.05 vs Ad-Null+AAB and Ad-Sh BNIP3+AAB, #*P*<0.05 vs Ad-Null. There was slight but significant decrease in LV end-systolic volume and increase in LVEF in the Ad-Sh BNIP3+AAB group, &*P*<0.05 vs Ad-Null+AAB. **F–I**, Pressure–volume loop measurements showed significant decreases in LV maximum pressure and LVEF and significant increases in left ventricular end-diastolic pressure (LVEDP) in the Ad-BNIP3+AAB group, **P*<0.05 vs Ad-Null+AAB and Ad-Sh BNIP3+AAB, #*P*<0.05 vs Ad-Null. There was significant decrease in LVEDP and a slight but significant increase in LVEF in the Ad-Sh BNIP3+AAB group, &*P*<0.05 vs Ad-Null+AAB. **J**, BNIP3 expression as well as cleaved caspase 3 significantly increased in the Ad-Null+AAB and was the highest in Ad-BNIP3+AAB, **P*<0.05 vs Ad-Null, #*P*<0.05 vs all other groups. BNIP3 knockdown significantly attenuated the increase in BNIP3 expression, cleaved caspase 3, and the conversion of LC3-1 to LC3-2 in response to pressure overload (PO), &*P*<0.05 vs Ad-Null+AAB and Ad-BNIP3+AAB. There was no difference in SERCA2a expression in all groups. **K**, Ultrastructurally, there was significant decrease in mitochondrial area 2 weeks after PO, **P*<0.05 vs Ad-Null and was the worst in Ad-BNIP3 group with significant mitochondrial fragmentation, cristae destruction, and myofibrillar damage, #*P*<0.05 vs all other groups. BNIP3 knockdown prevented mitochondrial damage in PO, &*P*<0.05 vs Ad-Null+AAB and Ad-BNIP3+AAB. **Arrows** are showing autophagosomes. Images ×5000 magnified, scale bar 2 µm. LV EDV indicates left ventricular end-diastolic volume; and LV ESV, left ventricular end-systolic volume.

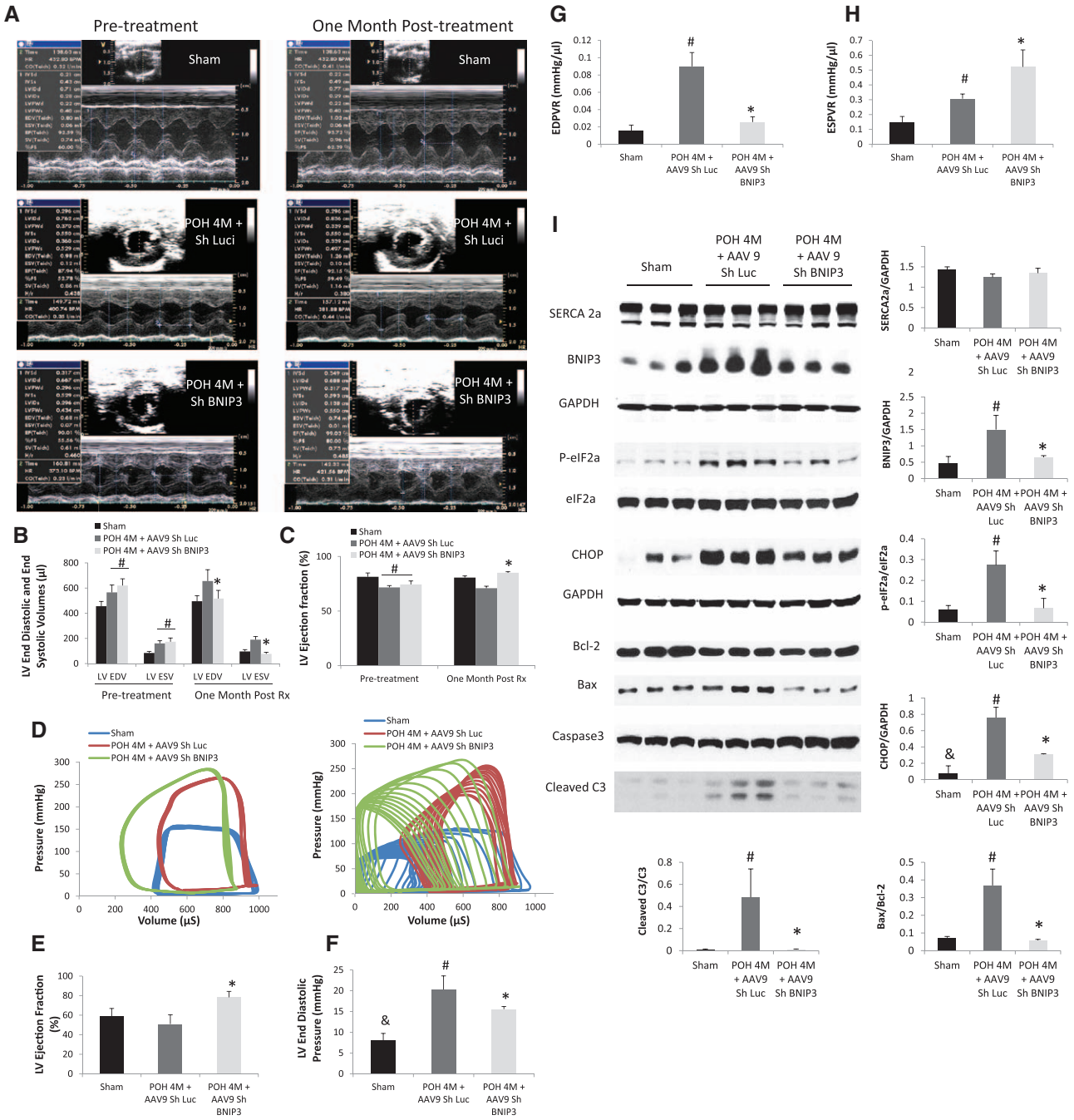

Figure 2. Tail vein delivery of 5E10 vg/mL of adeno-associated virus of serotype 9 (AAV9) Sh BNIP3 reversed cardiac remodeling and improved left ventricular (LV) diastolic function and contractility in a rat model of diastolic heart failure (HF) with preserved ejection fraction (EF). **A–C**, M-mode images of the above group of animals before and 1 month after treatment with AAV9 Sh Luc vs AAV9 Sh BNIP3. LV volumes were significantly decreased, and the LVEF was significantly increased 1 month after treatment with AAV9 Sh BNIP3, *P<0.05 vs pressure overload hypertrophy (POH) 4M+AAV9 Sh Luc, #P<0.05 vs sham. **D**, Pressure–volume loop tracings in the different groups at baseline and during inferior vena cava occlusion. **E**, LVEF significantly improved 1 month after Sh BNIP3 treatment, *P<0.05 vs other 2 groups. **F** and **G**, Left ventricular end-diastolic pressure (LVEDP) and end-diastolic pressure–volume relationship (EDPVR) were significantly increased in the Sh Luc group, #P<0.05 vs sham, &P<0.05 vs other 2 groups. Those parameters were significantly decreased 1 month after Sh BNIP3 treatment, *P<0.05 vs POH 4M+AAV9 Sh Luc. **H**, LV contractility significantly increased in the Sh BNIP3 group, *P<0.05 vs POH 4M+AAV9 Sh Luc. Note that the Sh Luc group has a falsely increased end-systolic pressure–volume relationship (ESPVR) compared with sham animals as their left ventricular end-systolic pressure (LVESP are higher, but their V0 is significantly shifted to the right as compared with the sham group). **I**, Western blot analysis of LV tissue lysate showed robust decrease in BNIP3 expression, endoplasmic reticulum (ER) stress (p-eIF2a), and ER stress apoptotic marker (CHOP [C/EBP homologous protein]), as well as in Bax/Bcl-2 ratio and in cleaved caspase 3 in the Sh BNIP3 group, P<0.05 vs POH 4M+AAV9 Sh Luc, #P<0.05 vs sham and &P<0.05 vs other 2 groups. There was no difference in SERCA2a expression among all groups.

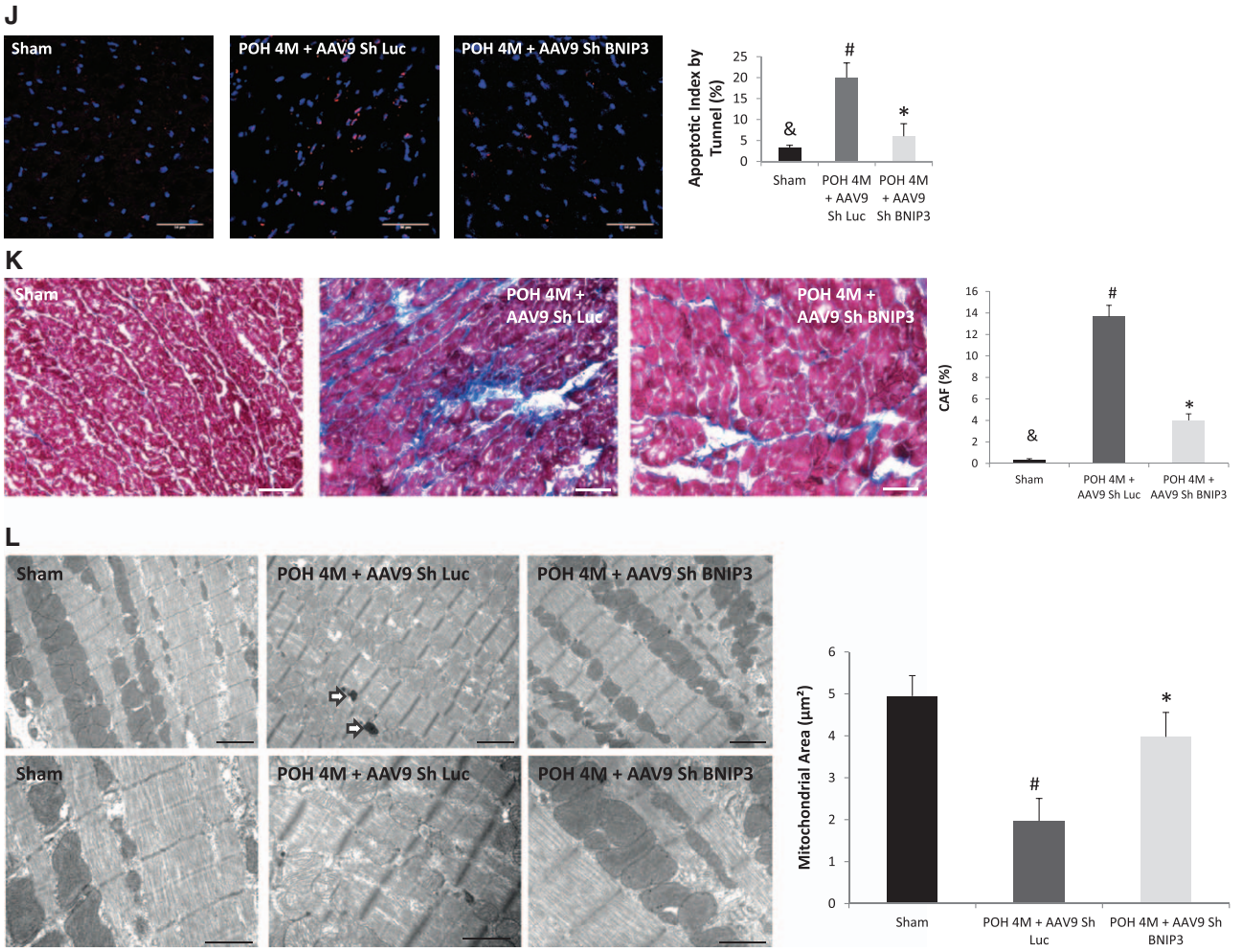

Figure 2 (Continued). **J** and **K**, There were robust decreases in myocardial apoptosis and in LV interstitial fibrosis in the Sh BNIP3 group, **P*<0.05 vs POH 4M+AAV9 Sh Luc, #*P*<0.05 vs sham and &*P*<0.05 vs other 2 groups. **L**, Ultrastructurally, there were significant mitochondrial fragmentation and cristae destruction with dilated T tubules and damaged myofibrils. BNIP3 knockdown robustly attenuated mitochondrial fragmentation and cristae destruction with the mitochondrial area almost back to control level and attenuated myofibrillar damage, #*P*<0.05 vs sham and **P*<0.05 vs POH 4M+AAV9 Sh Luc. **Arrows** showing the presence of autophagosomes. Above images are ×5000 magnified, scale bar 2 μm. Lower images are ×12 000 magnified, scale bar 1 μm. CAF indicates collagen area of fibrosis; LV EDV, left ventricular end-diastolic volume; and LV ESV, left ventricular end-systolic volume.

there are differences in each group in terms of mitochondria size, which may be because of the inhomogeneous nature of the gene transfer.

Therapeutic Gene Delivery of AAV9 Sh BNIP3 Reverses Cardiac Remodeling and Improves LV Diastolic and Systolic Function in a Pressure Overload–Induced HF Rat Model of Diastolic and Systolic Dysfunction

To examine the effects of knocking down BNIP3 in a chronic model of HF, we used AAV vectors that afford us long-term expression. Echocardiography data of the diastolic HF with preserved ejection fraction animals are shown in the Table III in the online-only Data Supplement. M-mode images are shown in Figure 2A. There were no significant differences in echocardiographic parameters between the Sh Luc and Sh BNIP3 groups before treatment. One month after treatment, there was significant decrease in LV end-systolic diameter and significant increase in LV fractional shortening in the AAV9 Sh BNIP3 group. LV end-diastolic and end-systolic volumes were significantly decreased because of the significant decrease in LV length in diastole and systole and reflected a significant increase in LVEF (Figure 2B and 2C; Figure IV in the online-only Data Supplement). Hemodynamic data are shown in Table IV in the online-only Data Supplement, and tracings are shown in Figure 2D. There were significant decreases in LV end-diastolic pressures and end-diastolic pressure–volume relationship and significant increases in LV ejection fraction and end-systolic pressure–volume relationship in the AAV9 Sh BNIP3 group (Figure 2E–2H). Western blotting of LV tissue lysate showed significant decreases in BNIP3 expression, as well as in Bax/Bcl-2 ratio, ER stress maker (p-eIF2a), and ER stress apoptotic marker (CHOP [C/EBP homologous protein]) and cleaved caspase 3 in the AAV9 Sh BNIP3 group (Figure 2I). However, there was no difference in SERCA2a expression between the AAV9 Sh Luc and AAV9 Sh BNIP3 groups, respectively (Figure 2I). Myocardial apoptosis and interstitial fibrosis were significantly decreased in the AAV9 Sh BNIP3

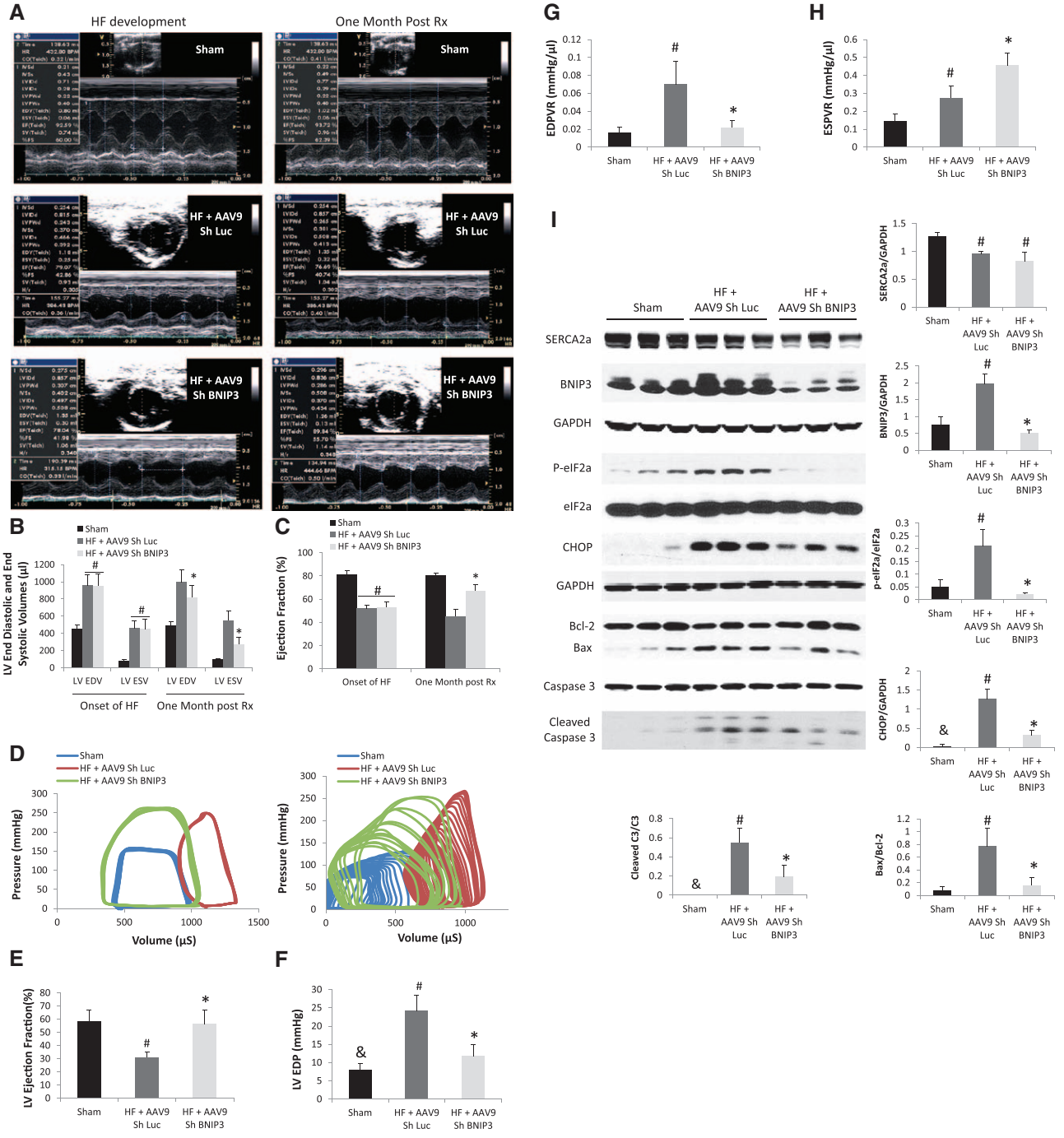

Figure 3. Tail vein delivery of 5E10 vg/mL of adeno-associated virus of serotype 9 (AAV9) Sh BNIP3 reversed cardiac remodeling and improved left ventricular (LV) diastolic function and contractility in a rat model of systolic heart failure (HF). **A**–**C**, M-mode images of the above group of animals before and 1 month after treatment with AAV9 Sh Luc vs AAV9 Sh BNIP3. LV volumes were significantly decreased, and the LV ejection fraction (EF) was significantly increased 1 month after treatment with AAV9 Sh BNIP3, **P*<0.05 vs HF+AAV9 Sh Luc, #*P*<0.05 vs sham. **D**, Pressure–volume loop tracings in the different groups at baseline and during inferior vena cava occlusion. **E**, LVEF significantly improved 1 month after Sh BNIP3 treatment, **P*<0.05 vs HF+AAV9 Sh Luc and #*P*<0.05 vs sham. **F** and **G**, Left ventricular end-diastolic pressure (LVEDP) and end diastolic pressure–volume relationship (EDPVR) were significantly increased in the Sh Luc group, #*P*<0.05 vs sham, &*P*<0.05 vs other 2 groups. Those parameters were significantly decreased 1 month after Sh BNIP3 treatment, **P*<0.05 vs HF+AAV9 Sh Luc. **H**, LV contractility significantly increased in the Sh BNIP3 group, **P*<0.05 vs HF+AAV9 Sh Luc. Note that the Sh Luc group has a falsely increased end-systolic pressure–volume relationship (ESPVR) compared with sham animals as their left ventricular end-systolic pressure (LVESP) are higher, but their V0 is significantly shifted to the right as compared with the sham group. **I**, Western blot analysis of LV tissue lysate showed robust decrease in BNIP3 expression, endoplasmic reticulum (ER) stress (p-eIF2a) and ER stress apoptotic marker (CHOP [C/EBP homologous protein]) as well as in Bax/Bcl-2 ratio and in cleaved caspase 3 in the Sh BNIP3 group, *P*<0.05 vs HF+AAV9 Sh Luc, #*P*<0.05 vs sham and &*P*<0.05 vs other 2 groups. There was a significant decrease in SERCA2a expression in the HF groups, #*P*<0.05 vs sham.

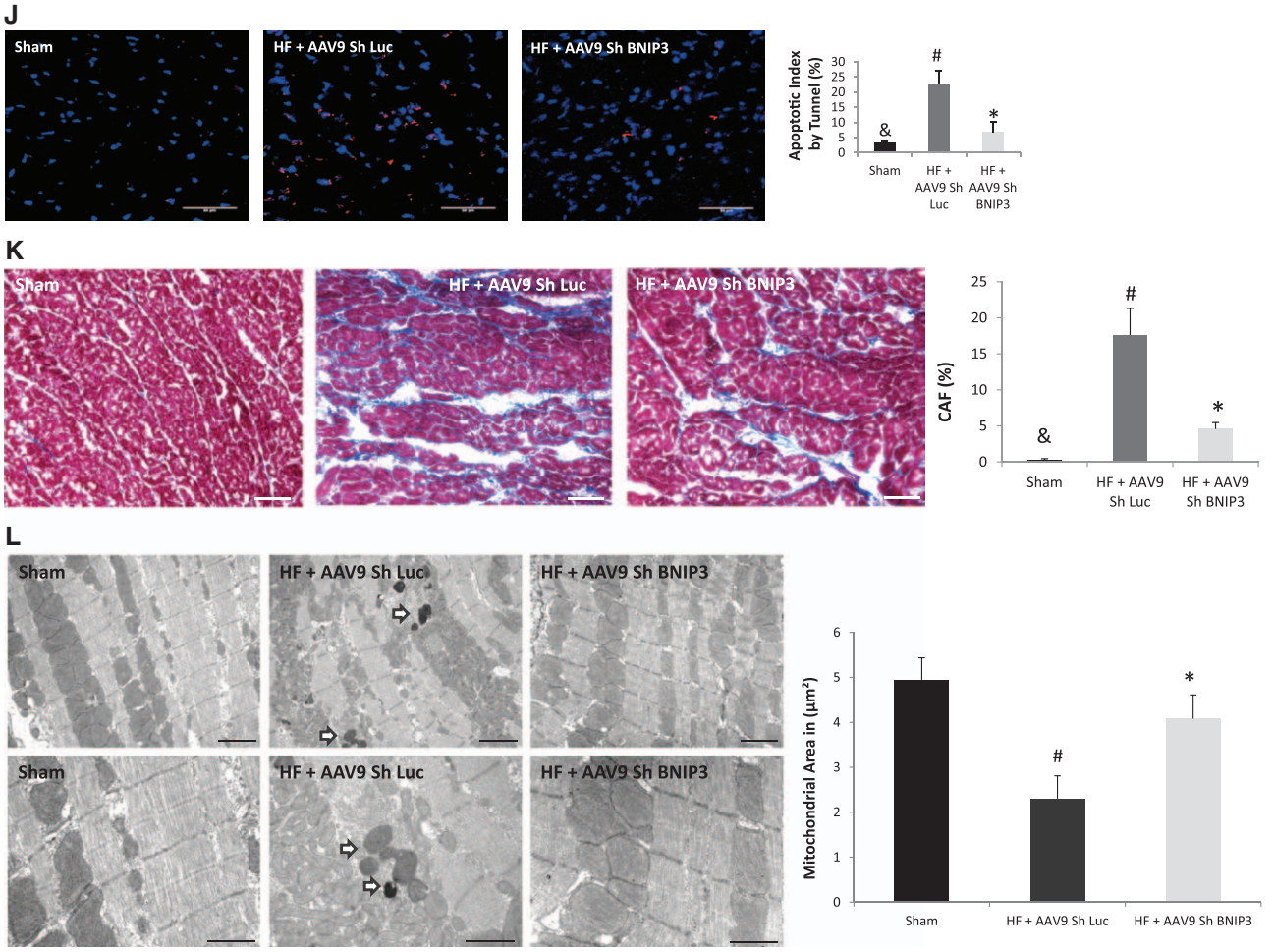

Figure 3 (Continued). **J** and **K**, There were robust decreases in myocardial apoptosis and in LV interstitial fibrosis in the Sh BNIP3 group, **P*<0.05 vs HF+AAV9 Sh Luc, #*P*<0.05 vs sham and &*P*<0.05 vs other 2 groups. **L**, Ultrastructurally, there was significant mitochondrial fragmentation and cristae destruction with dilated T tubules and damaged myofibrils. BNIP3 knockdown robustly attenuated mitochondrial fragmentation and cristae destruction with the mitochondrial area almost back to control level and attenuated myofibrillar damage, #*P*<0.05 vs sham and **P*<0.05 vs HF+AAV9 Sh Luc. **Arrows** showing the presence of autophagosomes. Above images are ×5000 magnified, scale bar 2 μm. Lower images are ×12 000 magnified, scale bar 1 μm. CAF indicates collagen area of fibrosis.

group (Figure 2J and 2K). Ultrastructurally, autophagosomes, mitochondrial fragmentation, and myofibrillar damage were noted in the AAV9 Sh Luc group. BNIP3 knockdown robustly improved the aforementioned ultrastructural findings (Figure 2L; Figure V in the online-only Data Supplement). Similar results were noted for the systolic HF animals treated with AAV9 Sh Luc versus AAV9 Sh BNIP3 except for that the systolic HF animals had much higher LV volumes and significantly lower SERCA2a expression compared with sham-operated animals (Figure 3I). Echocardiography and hemodynamic data are presented in Figure 3A–3H and Figure VI in the online-only Data Supplement, and Tables V and VI in the online-only Data Supplement. Myocardial apoptosis, interstitial fibrosis, and ultrastructure data are presented in Figure 3J–3L and Figure VII in the online-only Data Supplement.

Increase in BNIP3 Expression Decreases ER Calcium and Increases Mitochondrial Calcium

BNIP3 overexpressing cardiomyocytes had significantly decreased beat-to-beat Ca^{2+} release due to the significant decrease in ER Ca^{2+} with marked impairment in cardiomyocyte relaxation and 3-fold increase in mitochondrial Ca^{2+} (Figure 4A and 4B). Hypertrophic cardiomyocytes showed significant increase in beat-to-beat Ca^{2+} release and no change in ER Ca^{2+} content, 2 weeks after PO. However, 5 weeks after PO, beat-to-beat Ca^{2+} transients were significantly decreased attributable to a significant decrease in ER Ca^{2+} content. Beat-to-beat Ca^{2+} transients and ER Ca^{2+} content were significantly higher and mitochondrial Ca^{2+} was significantly lower in hypertrophic cardiomyocytes isolated from animals, 5 weeks after PO treated with AAB and tail vein injection of AAV9 Sh BNIP3 (Figure 4C and 4D).

BNIP3 Regulates Mitochondrial Calcium Via the Modulation of the VDAC Channels

Coimmunoprecipitation did not show a complex formation between BNIP3 and VDAC channels (Figure 5A). There was modulation of the VDAC channels by BNIP3. The increase in BNIP3 expression increases the oligomerization of the VDAC channels, mainly in the form of a dimer, with and without the presence of a cross-linking reagent, leading to

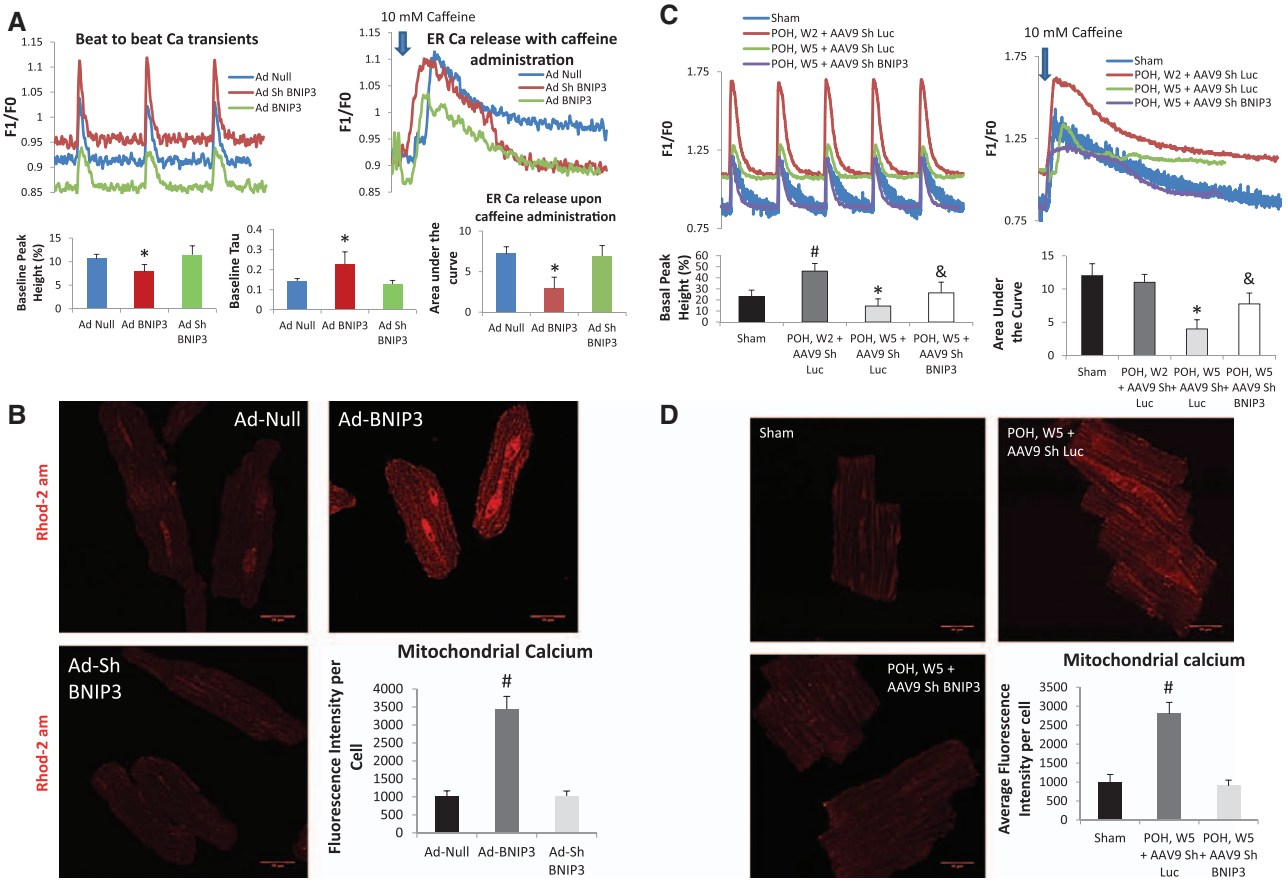

Figure 4. BNIP3 regulates endoplasmic reticulum (ER) and mitochondrial calcium homeostasis. **A**, BNIP3 overexpression in normal cardiomyocytes significantly decreased beat-to-beat Ca^{2+} release and ER Ca^{2+} content with significant increase in τ, **P*<0.05 vs Ad-Null and Ad-Sh BNIP3. There were no differences between the Ad-Null and Ad-Sh BNIP3 treated cardiomyocytes. **B**, There was 3-fold increase in mitochondrial Ca^{2+} in the Ad-BNIP3 group, **P*<0.05 vs Ad-Null and Ad-Sh BNIP3. **C**, In hypertrophic cardiomyocytes, there is robust increase in beat-to-beat Ca^{2+} release with no change in ER Ca^{2+} content 2 weeks after pressure overload (PO), #*P*<0.05 vs sham. However, 5 weeks after PO beat-to-beat Ca^{2+} transients are significantly decreased attributable to a significant decrease in ER Ca^{2+} content, **P*<0.05 vs all other groups. BNIP3 knockdown significantly increased beat-to-beat Ca^{2+} transients and ER Ca^{2+} content in hypertrophic cardiomyocytes 5 weeks after PO, &*P*<0.05 vs pressure overload hypertrophy (POH), W5+AAV9 Sh Luc. **D**, Mitochondrial Ca^{2+} significantly increased in hypertrophic cardiomyocytes 5 weeks after PO, #*P*<0.05 vs other 2 groups.

the increase in mitochondrial Ca^{2+} and to cytochrome C release (Figure 5B). DIDS (4,4'-diisothiocyanostilbene-2,2'-disulfonic acid), an anion channel inhibitor, inhibited the oligomerization of the VDAC channels and significantly attenuated mitochondrial Ca^{2+} and cell death in Ad-BNIP3–infected cardiomyocytes (Figure 5C–5E). Ultrastructurally, DIDS significantly attenuated mitochondrial fragmentation and autophagosome formation in Ad-BNIP3–infected cardiomyocytes. Overall, the mitochondrial area was significantly higher in cardiomyocytes treated with DIDS (Figure 5F; Figure VIII in the online-only Data Supplement).

Expression of a Constitutively Active FOXO3a Increases Cell Death In Vitro and Impairs Cardiac Diastolic and Systolic Function in a Rat Model of Early POH

Cardiomyocytes overexpressing constitutively active FOXO3a (Ad-FX3) showed significant increases in BNIP3 expression[10] and 4-fold increases in cell death (Figure IX in the online-only Data Supplement). Gene transfer of Ad-FX3 in a rat model of early POH was associated with a significantly lower body weight, LV weight, a significantly lower heart weight/body weight ratio and a significantly thinner septal and posterior wall by echocardiography (Figure 6A–6C; Table VII in the online-only Data Supplement). There were significant increases in LV end-systolic diameters and volumes and subsequently reflected significant decreases in LV fractional shortening and LVEF in the Ad-FX3+AAB group (Figure 6D and 6E). Baseline hemodynamics and tracing are shown in Table VIII in the online-only Data Supplement and Figure 6F, respectively. The Ad-FX3+AAB group had significant increase in their LV end-diastolic pressures, despite having a significantly lower maximum pressure and significant decrease in LVEF (Figure 6G–6I). On the molecular level, Ad-DN-FX3 significantly attenuated the increase in BNIP3 expression in response to PO (Figure 6J).

Discussion

BNIP3 is a mitochondrial death and mitophagy marker located at the outer mitochondrial membrane, with the N

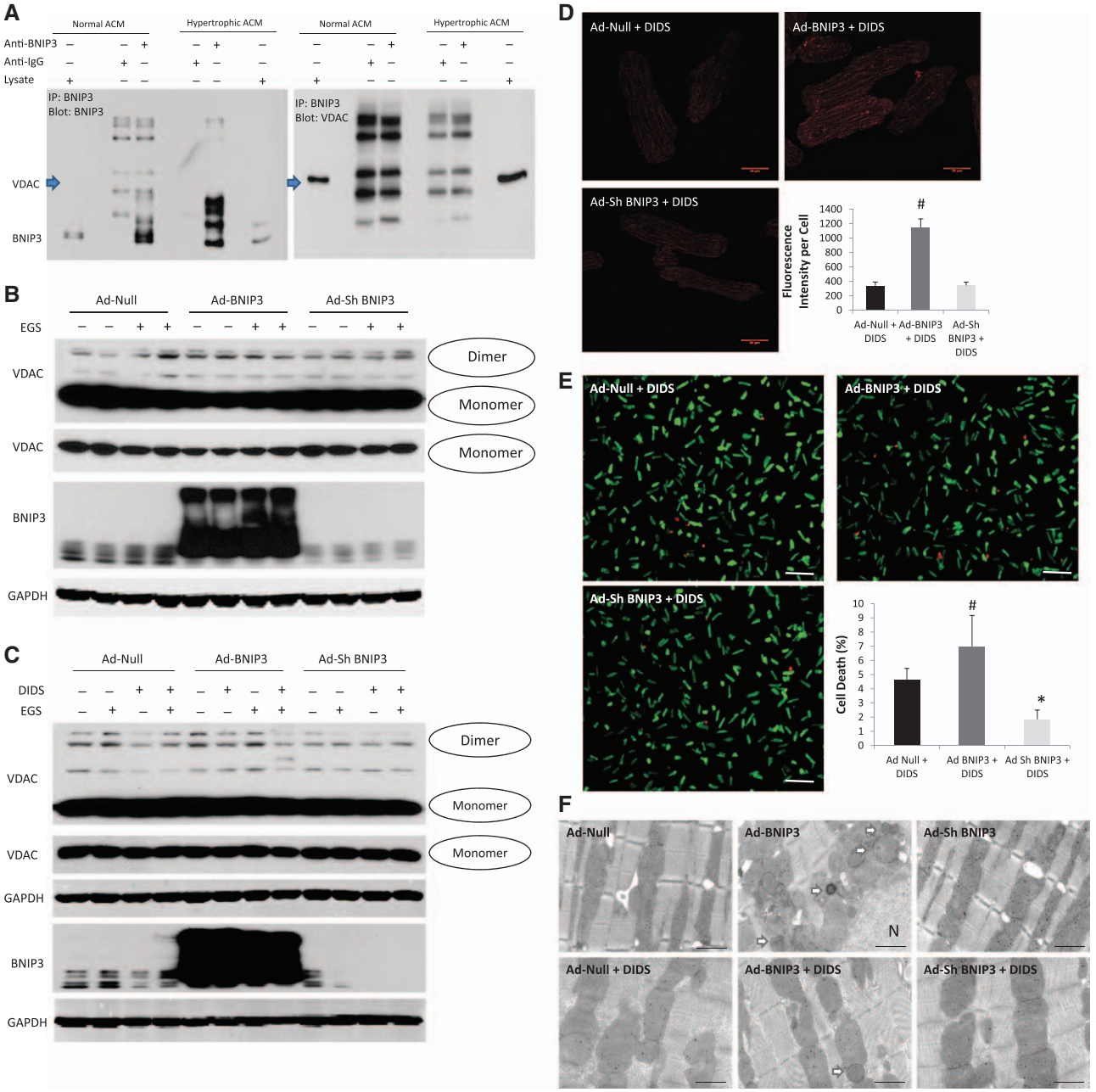

Figure 5. BNIP3 modulates the voltage-dependent anion channels (VDAC) and shifts the Ca from the endoplasmic reticulum (ER) into the mitochondria. **A**, Coimmunoprecipitation did not show that BNIP3 and VDAC channels form a complex. **B**, Rather there is modulation of the VDAC channels by BNIP3. The increase in BNIP3 expression causes oligomerization of the VDAC channels, mainly in the form of a dimer, with and without the presence of a cross-linking reagent (EGS) leading to the increase in mitochondrial Ca^{2+}. **C** and **D**, DIDS, an anion channel inhibitor, inhibited the oligomerization of the VDAC channels in Ad-BNIP3 infected cardiomyocytes. There was a 3-fold decrease in mitochondrial Ca^{2+} in all groups with significant decrease in the Ad-BNIP3 infected cardiomyocytes treated with DIDS, #P<0.05 vs Ad-Null+DIDS and Ad-Sh BNIP3+DIDS. **E**, DIDS significantly attenuated cell death in Ad-BNIP3 infected cardiomyocytes, #P<0.05 vs Ad-Null+DIDS and *P<0.05 vs other 2 groups. **F**, Ultrastructurally, DIDS significantly attenuated mitochondrial fragmentation and autophagosome formation in Ad-BNIP3 infected cardiomyocytes. The mitochondrial area was significantly higher in cardiomyocytes treated with DIDS compared with no DIDS treatment. Images ×12 000 magnified, scale bar 1 μm.

terminus oriented into the cytoplasm and the C terminus inside the mitochondria. It has been shown that an increase in BNIP3 expression under hypoxemic conditions increases cell death and mitochondrial autophagy and attributes to LV remodeling and myocardial apoptosis postmyocardial infarction.[1–4,6–9,21] Also, it has been shown how BNIP3 and NIX play a role in ER/SR-mitochondrial Ca^{2+} homeostasis.[22,23] In our previous study, we have shown that BNIP3 expression increases in POH and peaks at the time of HF development and highlighted the critical role of JNK in the modulation of FOXO3a for the expression of BNIP3. We also validated the JNK-FOXO3a-BNIP3 pathway in human samples of HF.[10] In this study, we show the critical role of BNIP3 in inducing LV remodeling and myocardial stiffness in PO rat model of

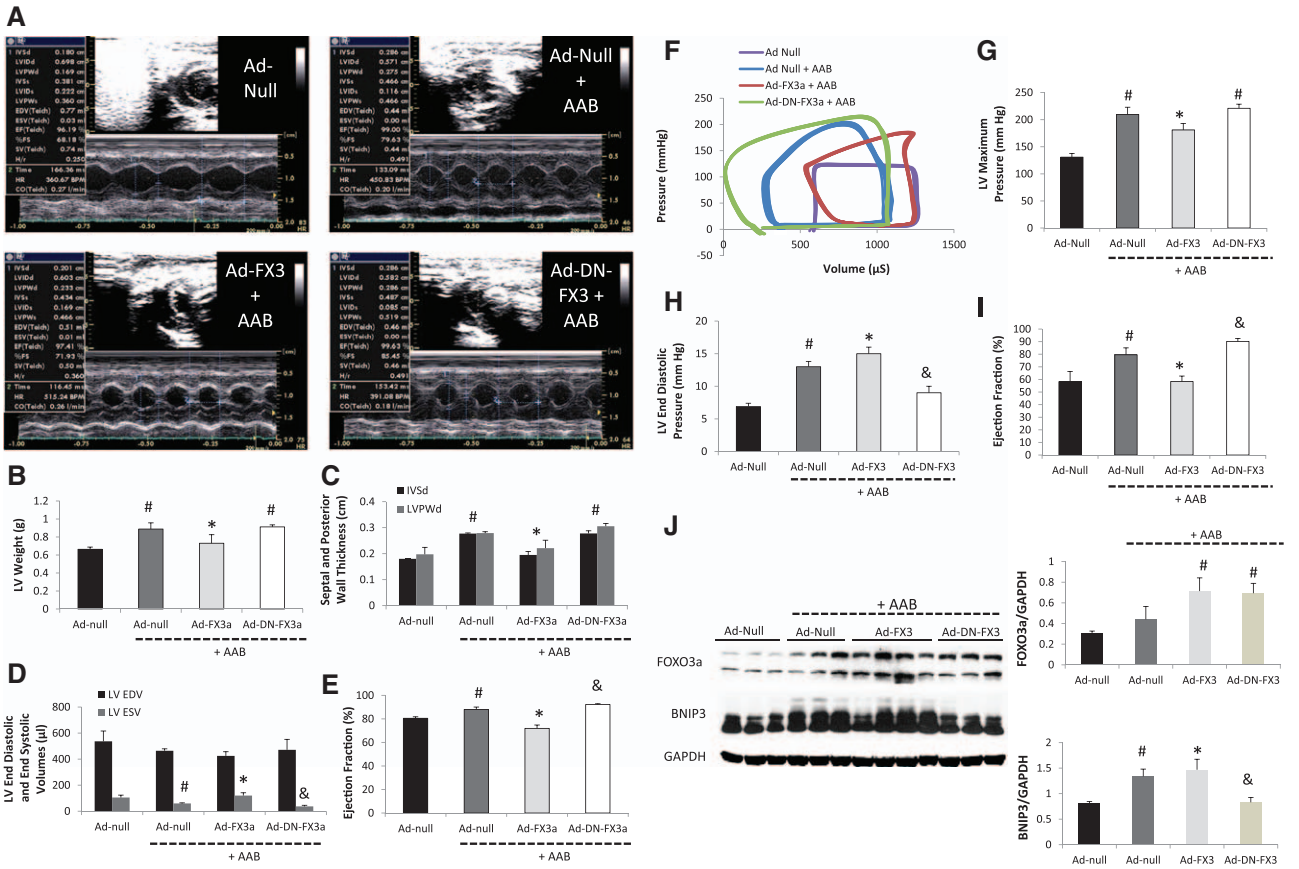

Figure 6. The expression of a constitutively active FOXO3a impairs cardiac diastolic and systolic function in a rat model of early pressure overload hypertrophy (POH). **A**, M-mode images 2 weeks after gene delivery via a cross-clamp technique and ascending aortic banding (AAB). **B–E**, There were significant decreases in left ventricular (LV) weight, interventricular septum thickness (IVSd), left ventricular end-diastolic posterior wall dimension (LVPWd), and LV ejection fraction (EF) and significant increase in LV end-systolic volume in the Ad-FX3a+AAB group, **P*<0.05 vs Ad-Null+AAB and Ad-DN-FX3a+AAB, #*P*<0.05 vs Ad-Null. There was slight but significant decrease in LV end-systolic volume (LVESV) and increase in LVEF in the Ad-DN-FX3+AAB group, &*P*<0.05 vs Ad-Null+AAB. **F–I**, Pressure–volume loop measurements showed significant decreases in LV maximum pressure and EF, and significant increases in left ventricular end-diastolic pressure (LVEDP) in the Ad-FX3a+AAB group, **P*<0.05 vs Ad-Null+AAB and Ad-DN-FX3a+AAB, #*P*<0.05 vs Ad-Null. There was significant decrease in LVEDP and a slight but significant increase in LVEF in the Ad-DN-FX3a+AAB group, &*P*<0.05 vs Ad-Null+AAB. **J**, FOXO3a expression increased in the Ad-FX3a and Ad-DN-FX3a groups, #*P*<0.05 vs Ad-Null and Ad-Null+AAB. BNIP3 expression increased in the Ad-Null+AAB and in the Ad-FX3a+AAB groups, #*P*<0.05 vs Ad-Null and **P*<0.05 vs all other groups. The delivery of Ad-DN-FX3a significantly attenuated the increase in BNIP3 expression in response to pressure overload, &*P*<0.05 vs Ad-Null+AAB and Ad-FX3a+AAB. LVEDV indicates LV end-diastolic volume.

HF, and we highlight a novel mechanism through which the chronic increase in BNIP3 expression induces mitochondrial damage, cytochrome C release, apoptosis, and thus myocardial fibrosis. In cardiac myocytes, BNIP3 is the effector of the transcription factor FOXO3a. The expression of constitutively active FOXO3a in cardiac myocytes, in vitro, was associated with significant increase in BNIP3 expression and cell death.[10] Gene transfer of constitutively active FOXO3a in a rat model of POH was associated with worsening in LV diastolic function and a decline in LV systolic function. Similar results were noted with the overexpression of BNIP3 in a rat model of early POH. BNIP3 knockdown by gene transfer of Ad-Sh BNIP3 robustly improved diastolic function and LV relaxation and significantly attenuated mitochondrial fragmentation in POH. Moreover, BNIP3 knockdown in 2 models of HF, a diastolic and a systolic dysfunction, was associated with significant decreases in LV end-diastolic and LV end-systolic volumes, myocardial apoptosis, and interstitial fibrosis, and a significant increase in LVEF. Hemodynamically, there were significant improvements in LV relaxation and contractility. Ultrastructurally, BNIP3 knockdown in HF markedly improved mitochondrial morphology and integrity with significant decrease in autophagosomes formation. From the results listed above, it seems that the chronic increase in BNIP3 expression mainly contributes to the diastolic dysfunction with moderate increases in LV volumes and decline in LVEF, as seen in the HF model of diastolic dysfunction. However, the full-blown dilatation and remodeling of the LV chamber with marked decline in LVEF is only seen when SERCA2a expression is downregulated along with an abnormally increased BNIP3 expression. This contributes to the significant decline in LV systolic function, fluid retention, and volume overload with major increases in LV end-diastolic and end-systolic volumes. We find that one of the mechanisms by which BNIP3 exerts these deleterious effects on the mitochondria is via the modulation of the VDAC channels. The increase in BNIP3 expression enhances the oligomerization of the VDAC channels shifting Ca^{2+} from the ER into the mitochondria.[24–27] DIDS, an anion channel inhibitor,

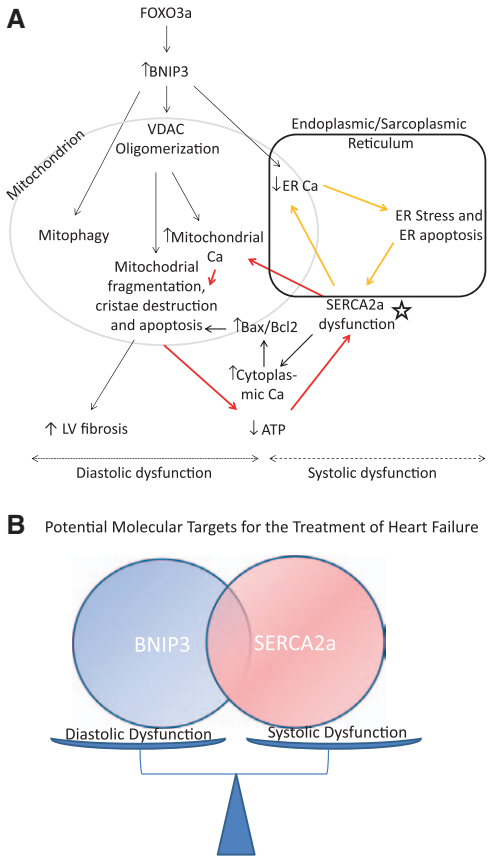

Figure 7. Schematic illustration of the mechanism by which BNIP3 induces mitochondrial damage and cell death. **A**, The increase in BNIP3 expression leads to the oligomerization of the voltage-dependent anion channel (VDAC) channels causing the shift in endoplasmic reticulum (ER) Ca^{2+} toward the mitochondria. This shift of ER Ca^{2+} has 2 sequelae, the first being the increase in mitochondrial Ca^{2+}, and the second is the decrease in ER Ca^{2+} content. The increase in mitochondrial Ca^{2+} leads to mitochondrial fragmentation, mitophagy, and apoptosis, decline in cardiac energetics, and left ventricular (LV) interstitial fibrosis (diastolic dysfunction), whereas, the decrease in ER Ca^{2+} leads to ER stress and ER stress–induced apoptosis (systolic dysfunction). In systolic heart failure (HF), SERCA2a downregulation (star), which is an independent process from the increase in BNIP3 expression, contributes to the further decline in ER Ca^{2+} and to the further increase in mitochondrial Ca^{2+}, leading to 2 vicious cycles and hence becomes the core of these 2 cycles as shown in the figure above (red and yellow arrows). **B**, Cartoon highlighting the interplay between BNIP3 and SERCA2a in modulating diastolic and systolic function of the cardiomyocyte, respectively.

attenuated VDAC oligomerization, mitochondrial damage, and cell death in BNIP3 overexpressing cardiomyocytes. The decrease in ER Ca^{2+} content creates an ER stress condition with significant increases in ER stress and ER stress apoptotic markers, p-eIF2a (phosphorylated Eukaryotic initiation factor) and CHOP, respectively. On the contrary, the increase in mitochondrial Ca^{2+} leads to their fragmentation, cristae destruction, and to the release of cytochrome C, either from the mPTP (mitochondrial permeability transition pore) or from the oligomers of the VDAC channels,[27] leading to the increase in myocardial apoptosis and LV interstitial fibrosis. Hence the stiffness of the myocardium seen with the increase in BNIP3 expression is a multifactorial process and to a large extent is clearly linked to mitochondrial calcium overload and decline in cardiac energetics, SERCA2a malfunction and to the increase in LV apoptosis and interstitial fibrosis. SERCA2a downregulation worsens the deleterious effect exerted by BNIP3 on the mitochondria, as well as ER stress, and becomes the core of 2 vicious cycles as shown in Figure 7. SERCA2a overexpression in systolic HF improved LV systolic function and attenuated BNIP3-mediated mitochondrial destruction and ER stress by shuffling the Ca^{2+} from the cytoplasm into the ER (Figure X in the online-only Data Supplement). The simultaneous overexpression of SERCA2a and BNIP3 in cardiomyocytes in vitro attenuated mitochondrial fragmentation compared with BNIP3 overexpression alone. However, DIDS was superior in preventing BNIP3-induced mitochondrial destruction in BNIP3 overexpressing cardiomyocytes. Morphologically, the largest mitochondria were seen in cardiomyocytes in vitro by simultaneous overexpression of SERCA2a and BNIP3 knockdown and with BNIP3 knockdown plus DIDS treatment (Figure X in the online-only Data Supplement).

In conclusion, the increase in BNIP3 expression, which is highest in HF, primarily contributes to diastolic dysfunction through the intracellular destruction exerted by BNIP3 on the mitochondria leading to mitophagy, apoptosis, decline in cardiac energetics and myocardial fibrosis, and stiffness, and to the systolic dysfunction via the ER-mitochondria Ca^{2+} shift, and decline in ER Ca^{2+} content. However, the major remodeling of the LV chamber, which is seen in systolic HF, takes place when SERCA2a expression is downregulated, which along with the increase in BNIP3 expression contribute to the systolic and diastolic dysfunction of the cardiomyocyte with significant increases in LV end-diastolic and end-systolic volumes and significant decline in LV contractile function and LVEF.

Acknowledgments

Statistical revision was conducted via the support of National Institutes of Health grant UL1TR000067 by Dr Bagiella Emilia.

Sources of Funding

This work is supported by National Institutes of Health R01 HL083156, HL080498, HL093183, and P20HL100396 to Dr Hajjar and by a 2011 Research Fellowship Award from the Heart Failure Society of America to Dr Chaanine.

Disclosures

A patent application has been submitted for this work.

References

1. Diwan A, Krenz M, Syed FM, Wansapura J, Ren X, Koesters AG, Li H, Kirshenbaum LA, Hahn HS, Robbins J, Jones WK, Dorn GW. Inhibition of ischemic cardiomyocyte apoptosis through targeted ablation of Bnip3 restrains postinfarction remodeling in mice. *J Clin Invest*. 2007;117:2825–2833.
2. Dorn GW 2nd. Mitochondrial pruning by Nix and BNip3: an essential function for cardiac-expressed death factors. *J Cardiovasc Transl Res*. 2010;3:374–383.
3. Gang H, Hai Y, Dhingra R, Gordon JW, Yurkova N, Aviv Y, Li H, Aguilar F, Marshall A, Leygue E, Kirshenbaum LA. A novel hypoxia-inducible spliced variant of mitochondrial death gene Bnip3 promotes survival of ventricular myocytes. *Circ Res*. 2011;108:1084–1092.
4. Kubli DA, Quinsay MN, Huang C, Lee Y, Gustafsson AB. Bnip3 functions as a mitochondrial sensor of oxidative stress during myocardial ischemia and reperfusion. *Am J Physiol Heart Circ Physiol*. 2008;295:H2025–H2031.

5. Landes T, Emorine LJ, Courilleau D, Rojo M, Belenguer P, Arnauné-Pelloquin L. The BH3-only Bnip3 binds to the dynamin Opa1 to promote mitochondrial fragmentation and apoptosis by distinct mechanisms. *EMBO Rep*. 2010;11:459–465.
6. Quinsay MN, Lee Y, Rikka S, Sayen MR, Molkentin JD, Gottlieb RA, Gustafsson AB. Bnip3 mediates permeabilization of mitochondria and release of cytochrome c via a novel mechanism. *J Mol Cell Cardiol*. 2010;48:1146–1156.
7. Quinsay MN, Thomas RL, Lee Y, Gustafsson AB. Bnip3-mediated mitochondrial autophagy is independent of the mitochondrial permeability transition pore. *Autophagy*. 2010;6:855–862.
8. Regula KM, Ens K, Kirshenbaum LA. Inducible expression of BNIP3 provokes mitochondrial defects and hypoxia-mediated cell death of ventricular myocytes. *Circ Res*. 2002;91:226–231.
9. Zhang J, Ney PA. Role of BNIP3 and NIX in cell death, autophagy, and mitophagy. *Cell Death Differ*. 2009;16:939–946.
10. Chaanine AH, Jeong D, Liang L, Chemaly ER, Fish K, Gordon RE, Hajjar RJ. JNK modulates FOXO3a for the expression of the mitochondrial death and mitophagy marker BNIP3 in pathological hypertrophy and in heart failure. *Cell Death Dis*. 2012;3:265.
11. Piper HM, Probst I, Schwartz P, Hütter FJ, Spieckermann PG. Culturing of calcium stable adult cardiac myocytes. *J Mol Cell Cardiol*. 1982;14:397–412.
12. Wold LE, Ren J. Mechanical measurement of contractile function of isolated ventricular myocytes. *Methods Mol Med*. 2007;139:263–270.
13. Kim M, Oh JK, Sakata S, Liang I, Park W, Hajjar RJ, Lebeche D. Role of resistin in cardiac contractility and hypertrophy. *J Mol Cell Cardiol*. 2008;45:270–280.
14. Suckau L, Fechner H, Chemaly E, Krohn S, Hadri L, Kockskämper J, Westermann D, Bisping E, Ly H, Wang X, Kawase Y, Chen J, Liang L, Sipo I, Vetter R, Weger S, Kurreck J, Erdmann V, Tschope C, Pieske B, Lebeche D, Schultheiss HP, Hajjar RJ, Poller WC. Long-term cardiac-targeted RNA interference for the treatment of heart failure restores cardiac function and reduces pathological hypertrophy. *Circulation*. 2009;119:1241–1252.
15. Del Monte F, Butler K, Boecker W, Gwathmey JK, Hajjar RJ. Novel technique of aortic banding followed by gene transfer during hypertrophy and heart failure. *Physiol Genomics*. 2002;9:49–56.
16. Hajjar RJ, Schmidt U, Matsui T, Guerrero JL, Lee KH, Gwathmey JK, Dec GW, Semigran MJ, Rosenzweig A. Modulation of ventricular function through gene transfer in vivo. *Proc Natl Acad Sci USA*. 1998;95:5251–5256.
17. del Monte F, Hajjar RJ. Efficient viral gene transfer to rodent hearts in vivo. *Methods Mol Biol*. 2003;219:179–193.
18. Pacher P, Nagayama T, Mukhopadhyay P, Bátkai S, Kass DA. Measurement of cardiac function using pressure-volume conductance catheter technique in mice and rats. *Nat Protoc*. 2008;3:1422–1434.
19. Porterfield JE, Kottam AT, Raghavan K, Escobedo D, Jenkins JT, Larson ER, Treviño RJ, Valvano JW, Pearce JA, Feldman MD. Dynamic correction for parallel conductance, GP, and gain factor, alpha, in invasive murine left ventricular volume measurements. *J Appl Physiol*. 2009;107:1693–1703.
20. Baan J, van der Velde ET, de Bruin HG, Smeenk GJ, Koops J, van Dijk AD, Temmerman D, Senden J, Buis B. Continuous measurement of left ventricular volume in animals and humans by conductance catheter. *Circulation*. 1984;70:812–823.
21. Gustafsson AB. Bnip3 as a dual regulator of mitochondrial turnover and cell death in the myocardium. *Pediatr Cardiol*. 2011;32:267–274.
22. Diwan A, Matkovich SJ, Yuan Q, Zhao W, Yatani A, Brown JH, Molkentin JD, Kranias EG, Dorn GW 2nd. Endoplasmic reticulum-mitochondria crosstalk in NIX-mediated murine cell death. *J Clin Invest*. 2009;119:203–212.
23. Zhang L, Li L, Liu H, Borowitz JL, Isom GE. BNIP3 mediates cell death by different pathways following localization to endoplasmic reticulum and mitochondrion. *FASEB J*. 2009;23:3405–3414.
24. Keinan N, Tyomkin D, Shoshan-Barmatz V. Oligomerization of the mitochondrial protein voltage-dependent anion channel is coupled to the induction of apoptosis. *Mol Cell Biol*. 2010;30:5698–5709.
25. Rapizzi E, Pinton P, Szabadkai G, Wieckowski MR, Vandecasteele G, Baird G, Tuft RA, Fogarty KE, Rizzuto R. Recombinant expression of the voltage-dependent anion channel enhances the transfer of Ca2+ microdomains to mitochondria. *J Cell Biol*. 2002;159:613–624.
26. Rizzuto R, Marchi S, Bonora M, Aguiari P, Bononi A, De Stefani D, Giorgi C, Leo S, Rimessi A, Siviero R, Zecchini E, Pinton P. Ca(2+) transfer from the ER to mitochondria: when, how and why. *Biochim Biophys Acta*. 2009;1787:1342–1351.
27. Shoshan-Barmatz V, De Pinto V, Zweckstetter M, Raviv Z, Keinan N, Arbel N. VDAC, a multi-functional mitochondrial protein regulating cell life and death. *Mol Aspects Med*. 2010;31:227–285.

CLINICAL PERSPECTIVE

Heart failure (HF), is a syndrome with complex pathophysiological disturbances and with major alterations in myocardial signaling pathways leading to changes in calcium handling proteins, mitochondrial dysfunction, and heightened levels of myocardial apoptotic and autophagic cell death. Moreover, although there is a clear mortality benefit with β-blockers, angiotensin-converting enzyme inhibitors and mineralocorticoid receptor antagonists in systolic HF, no therapies have shown promise in treating diastolic HF with preserved ejection fraction in different randomized clinical trials. In this study, we showed that the increase in BNIP3 expression correlated with diastolic dysfunction, mitochondrial apoptosis, and autophagy that were evident as early as 2 weeks after pressure overload hypertrophy. Those parameters worsened with BNIP3 overexpression, in vivo, and peaked at HF development, whether diastolic or systolic. The downregulation of SERCA2a contributed to worsening in left ventricular systolic function and cardiac remodeling leading to systolic HF. BNIP3 knockdown in HF robustly improved left ventricular end-diastolic pressure, myocardial relaxation, myocardial contractility, and cardiac remodeling, and significantly decreased myocardial apoptosis, and left ventricular interstitial fibrosis. The effects of increased BNIP3 expression on cardiomyocyte diastolic dysfunction is mediated by the calcium shift from the endoplasmic reticulum to the mitochondria, leading to mitochondrial calcium overload, mitochondrial dysfunction, and decline in cardiac energetics. This study highlights a novel role of BNIP3 as a potential therapeutic target for the treatment of diastolic HF.